Virology 405 (2010) 70–80

Contents lists available at ScienceDirect

Virology

journal homepage: www.elsevier.com/locate/yviro

Switch to high-level virus replication and HLA class I upregulation in differentiating megakaryocytic cells after infection with pathogenic hantavirus

Nina Lütteke [a], Martin J. Raftery [a], Pritesh Lalwani [a], Min-Hi Lee [a], Thomas Giese [d], Sebastian Voigt [b], Norbert Bannert [b], Harald Schulze [c], Detlev H. Krüger [a], Günther Schönrich [a,*]

[a] Institute of Medical Virology, Charité-Universitätsmedizin Berlin, Berlin, Germany
[b] Robert-Koch-Institute, Berlin, Germany
[c] Department of Pediatrics, Laboratory of Pediatric Molecular Biology, Charité-Universitätsmedizin Berlin, Berlin, Germany
[d] Institute of Immunology, University of Heidelberg, Heidelberg, Germany

ARTICLE INFO

Article history:
Received 16 February 2010
Returned to author for revision
26 March 2010
Accepted 22 May 2010
Available online 17 June 2010

Keywords:
Hantaviruses
Megakaryocytes
Innate immunity
Immunopathogenesis
HLA class I
Platelets
Viral hemorrhagic fever

ABSTRACT

Hantaan virus (HTNV), the prototype member of the *Hantavirus* genus in the family Bunyaviridae, causes hemorrhagic fever with renal syndrome (HFRS) in humans. Hemorrhage is due to endothelial barrier damage and a sharp decrease in platelet counts. The mechanisms underlying HTNV-associated acute thrombocytopenia have not been elucidated so far. Platelets are produced by mature megakaryocytes that develop during megakaryopoiesis. In this study, we show that HTNV targets megakaryocytic cells whereas rather non-pathogenic hantaviruses did not infect this cell type. After induction of differentiation megakaryocytic cells switched from low-level to high-level HTNV production without reduction in cell survival or alteration in differentiation. However, increased HTNV replication resulted in strong upregulation of HLA class I molecules although HTNV escaped type I interferon (IFN)-associated innate responses. Taken together, HTNV efficiently replicates in differentiating megakaryocytic cells resulting in upregulation of HLA class I molecules, the target structures for cytotoxic T cells (CTLs).

Introduction

Hantaviruses are enveloped negative-sense RNA viruses belonging to the family Bunyaviridae. They have co-evolved with rodent and insectivore species, their natural reservoir hosts (Schmaljohn and Nichol, 2007). In recent years, pathogenic hantaviruses emerged as an increasing threat to human health (Schmaljohn and Hjelle, 1997). Transmission can occur when humans inhale aerosols of excreta derived from chronically infected rodents. Different hantaviruses show different degrees of virulence in humans. For example, Prospect Hill virus (PHV) and Tula virus (TULV) are regarded as rather non-pathogenic to humans whereas Puumala virus (PUUV) causes nephropathia epidemica (NE), a relatively mild form of disease with a case fatality rate of less than 1%. Some hantavirus species in the Americas are associated with hantavirus cardiopulmonary syndrome (HCPS) with a case fatality rate of up to 45%. In Asia, Hantaan virus (HTNV), the prototype member of the genus *Hantavirus*, can elicit hemorrhagic fever with renal syndrome (HFRS) with a case fatality rate up to 15% (Kruger et al., 2001).

All hantavirus-associated syndromes have in common increased microvascular permeability as well as platelet dysfunction and a dramatic decrease in platelet counts at the beginning of vascular leakage and the hypotensive phase (Cosgriff, 1991; Cosgriff et al., 1991; Lee, 1987). At this critical stage, patients may die of irreversible shock. The underlying pathophysiological mechanisms are not yet understood. Hantaviruses are non-lytic viruses that do not cause cytopathic effects. It is well known that both pathogenic and non-pathogenic hantaviruses infect endothelial cells, which form a barrier at the interface of blood and tissue (Hippenstiel and Suttorp, 2003). Hantavirus infection does not induce cell death (Pensiero et al., 1992; Temonen et al., 1993; Yanagihara and Silverman, 1990; Zaki et al., 1995). Moreover, hantavirus infection per se is not sufficient to increase the permeability of endothelial cell monolayers *in vitro* (Khaiboullina et al., 2000; Sundstrom et al., 2001; Gavrilovskaya et al., 2008). This points toward immunopathogenesis playing an important role in virus-induced vascular injury (Schonrich et al., 2008). Even healthy individuals develop small vascular lesions that require adequate platelet function for repair (Kaushansky, 2005). Consequently, the lack of functional platelets which precedes the development of shock symptoms (Chang et al., 2007) is an important factor in hantaviral pathogenesis.

Mature megakaryocytes release platelets into the circulation (Schulze and Shivdasani, 2005) and are themselves derived from pluripotent hematopoietic stem cells which serve as lifelong source of

* Corresponding author. Mailing address: Institute of Medical Virology, Charité-Universitätsmedizin Berlin, Charitéplatz 1, D-10117 Berlin, Germany. Fax: +49 30 450 525 907.
E-mail address: guenther.schoenrich@charite.de (G. Schönrich).

0042-6822/$ – see front matter © 2010 Elsevier Inc. All rights reserved.
doi:10.1016/j.virol.2010.05.028

all circulating blood cells (Ogawa, 1993). The development of mature megakaryocytes (megakaryopoiesis) is characterized by commitment of multipotent stem cells to the megakaryocyte lineage, proliferation of progenitor cells, and terminal megakaryocyte differentiation. During a process called endoreplication (Edgar and Orr-Weaver, 2001), megakaryocytes become polyploid, multilobulated cells containing a large cytoplasmic mass. In terminal megakaryocyte differentiation, interactions between integrin receptors on the cell surface and extracellular matrix molecules such as fibronectin play a role (Berthier et al., 1998; Jiang et al., 2002). So far, it has not been investigated whether hantaviruses target megakaryocytes.

In this study, we investigated whether human megakaryocytic cells are susceptible to hantavirus infection and analyze its phenotypic and functional implications.

Results

Expression of hantavirus receptors on human megakaryocytic cell lines and human primary megakaryocytes

Primary megakaryocytes constitute only 0.03–0.06% of all nucleated cells in the bone marrow and are difficult to isolate (Saito, 1997). Therefore, we used human megakaryocytic cell lines to investigate the interaction between hantaviruses and megakaryocytes. Initially, the expression of hantavirus receptors on the surface of established megakaryocytic cell lines was assessed by using flow cytometry and compared to human primary megakaryocytes. Fig. 1 shows that similar to human primary megakaryocytes the human megakaryocytic cell lines HEL, K562, Meg-01, and TF-1 cells strongly expressed CD29 (integrin β1), the receptor for non-pathogenic hantaviruses (Gavrilovskaya et al., 1998, 1999). In contrast, CD61 (integrin β3), an important receptor component for pathogenic hantaviruses such as HTNV (Gavrilovskaya et al., 1999), was efficiently expressed by HEL cells and human primary megakaryocytes. This important molecule was found to a much lesser extent on TF-1 or Meg-01 cells and was not detectable on K562 cells. A high density of decay-accelerating factor (DAF or CD55), another molecule involved in hantavirus infection (Krautkramer and Zeier, 2008), was observed on all cell lines and was strongly expressed on human primary megakaryocytes. However, the receptor for the globular head domain of complement component C1q (gC1qR), also recently identified as a receptor component for HTNV (Choi et al., 2008), was found on none of these megakaryocytic cell lines whereas relatively weak expression was detected on human primary megakaryocytes.

In conclusion, from all human megakaryocytic cell lines tested, HEL cells showed the strongest expression of entry receptors for hantaviruses and resembled in this regard human primary megakaryocytes.

Susceptibility of human megakaryocytic cell lines and human primary megakaryocytes to hantavirus infection

We further analyzed the susceptibility of HEL cells to hantavirus infection. These cells represent a well-established model system for

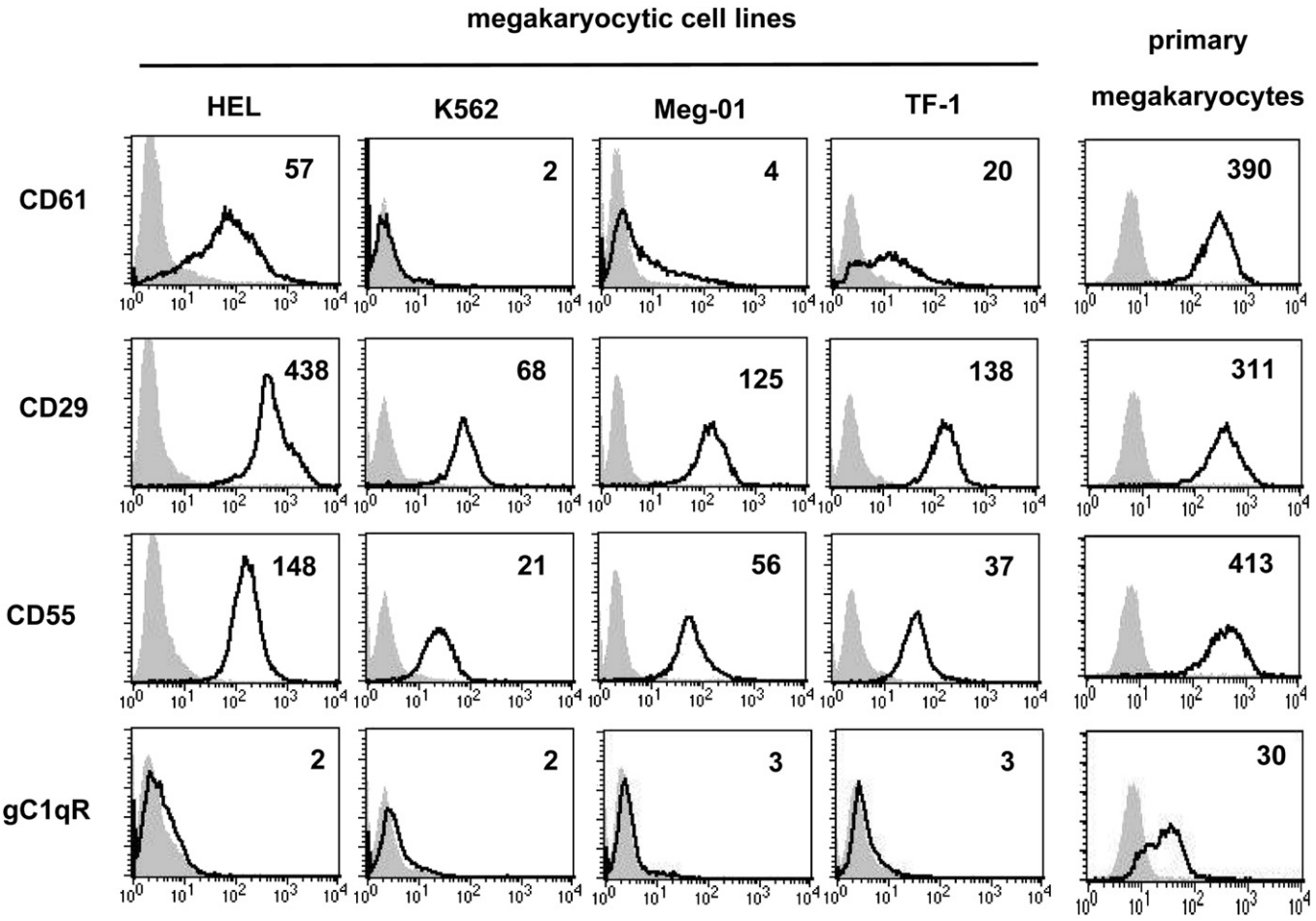

Fig. 1. Expression of cellular receptors for hantaviruses on human megakaryocytic cells and human primary megakaryocytes. Cells were stained with primary antibodies specific for CD29 (integrin β1), CD61 (integrin β3), CD55/DAF, or gC1qR. As secondary antibody PE-conjugated anti-mouse IgG was used. Grey filled histograms represent isotype controls, and black histograms show specific staining as indicated. The mean fluorescence intensity (MFI) is given in the upper right corner. On the *x*-axis, the fluorescence intensity (log scale, 4 decades) is given, whereas the *y*-axis depicts cell counts.

studying megakaryopoiesis (Long et al., 1990). After treatment with phorbol 12-myristate 13-acetate (PMA), HEL cells further differentiate along the megakaryocytic lineage. Fluorescence-labeled fibrinogen did not stain HEL cells (data not shown), indicating that integrin receptor αIIbβ3 is in an inactive conformation. This allows pathogenic hantaviruses such as HTNV to bind to the N-terminal plexin–semaphorin–integrin (PSI) domain of β3 (Raymond et al., 2005). Indeed, viral N protein could be detected in HEL cells inoculated with HTNV by using immunofluorescence microscopy (Fig. 2A). Intriguingly, after induction of HEL cell differentiation with PMA, expression of viral N protein in HTNV-infected HEL cell cultures was drastically increased. In contrast, both unstimulated and PMA-stimulated cell cultures inoculated with PHV or TULV remained negative for viral antigen. Confocal laser scanning microscopy confirmed the presence of viral N protein in the cytoplasm of HTNV-infected HEL cells (Fig. 2B). Moreover, human primary megakaryocytes were susceptible to HTNV infection (Fig. 2C). Finally, the HTNV N protein was detected in unstimulated and PMA-stimulated HEL cells after HTNV infection by Western blot analysis (Fig. 2D).

Taken together, these results demonstrate that HTNV but not TULV or PHV, which are rather non-pathogenic, targets megakaryocytic cells.

Switch to high-level HTNV replication in differentiating megakaryocytic cells

We investigated in more detail the impact of PMA-induced megakaryocyte differentiation on cell proliferation and viral replication. Stimulation with PMA was associated with an arrest in cell proliferation of both mock-infected (Fig. 3A) and HTNV-infected (Fig. 3B) HEL cells. As shown in Fig. 3C HTNV replicated with moderate efficiency in untreated HEL cells reaching titers of approximately 10^3 FFU/ml. We also observed low-level HTNV production in untreated TF-1 cells (data not shown). Intriguingly, a switch from low-level to high-level virion production occurred after PMA-induced megakaryocyte differentiation despite of cell proliferation arrest. The HTNV titers increased more than 100-fold and reached peak titers between 10^5 and 10^6 FFU/ml, only slightly less than the peak titers usually found in HTNV-infected Vero E6 cell cultures. Moreover, enhanced output of infectious particles in PMA-treated HEL cells was observed whether PMA was added 1 day before or 1 h post-HTNV infection (Fig. 3D, left panel). The increased HTNV titers observed for PMA-treated HEL cells could have been due to residual PMA in viral supernatant. This could have boosted viral replication in Vero E6 cells which are routinely used for virus titration. To exclude this possibility, Vero E6 cells were infected with HTNV and stimulated with PMA. In contrast to HEL cells, PMA did not enhance

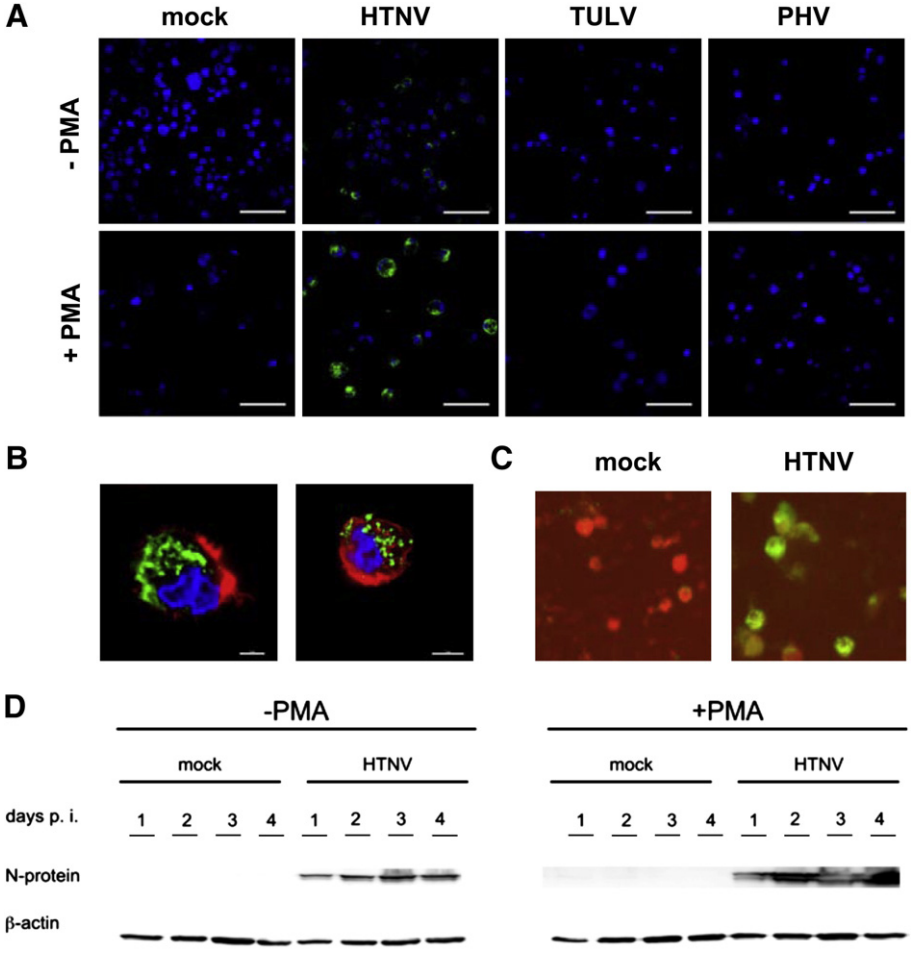

Fig. 2. Detection of viral N protein in hantavirus-infected HEL cells and human primary megakaryocytes. (A) Immunofluorescence microscopy analysis of mock- or hantavirus-infected (MOI = 1.5) HEL cells that were left unstimulated (−PMA) or stimulated (10 nM PMA at 1 h p.i.). At 3 days p.i., cells were stained for viral N protein (green) and nuclei (blue) before analysis. (bar = 50 μm) (B) Confocal laser scanning microscopy showing typical N protein patterns in HTNV-infected (MOI = 1.5) HEL cells that were stimulated (10 nM PMA at 1 h p.i.) and stained at 3 days p.i. for viral N protein (green), F-actin (red), and DNA (blue) before analysis. (bar = 5 μm). (C) Immunofluorescence microscopy analysis of human primary megakaryocytes that were mock-infected or infected with HTNV (MOI = 1.5) and stimulated (10 nM PMA at 1 h p.i.). Cells were stained 3 days p.i. for viral N protein (green) and CD61 (red). (D) Western blot analysis of mock- or HTNV-infected HEL cells (MOI = 1.5) that were left untreated (−PMA) or stimulated (10 nM PMA at 1 h p.i.) and analyzed for viral N protein expression at day 1, 2, 3, and 4 p.i. as indicated. As loading control, the amount of β-actin was determined.

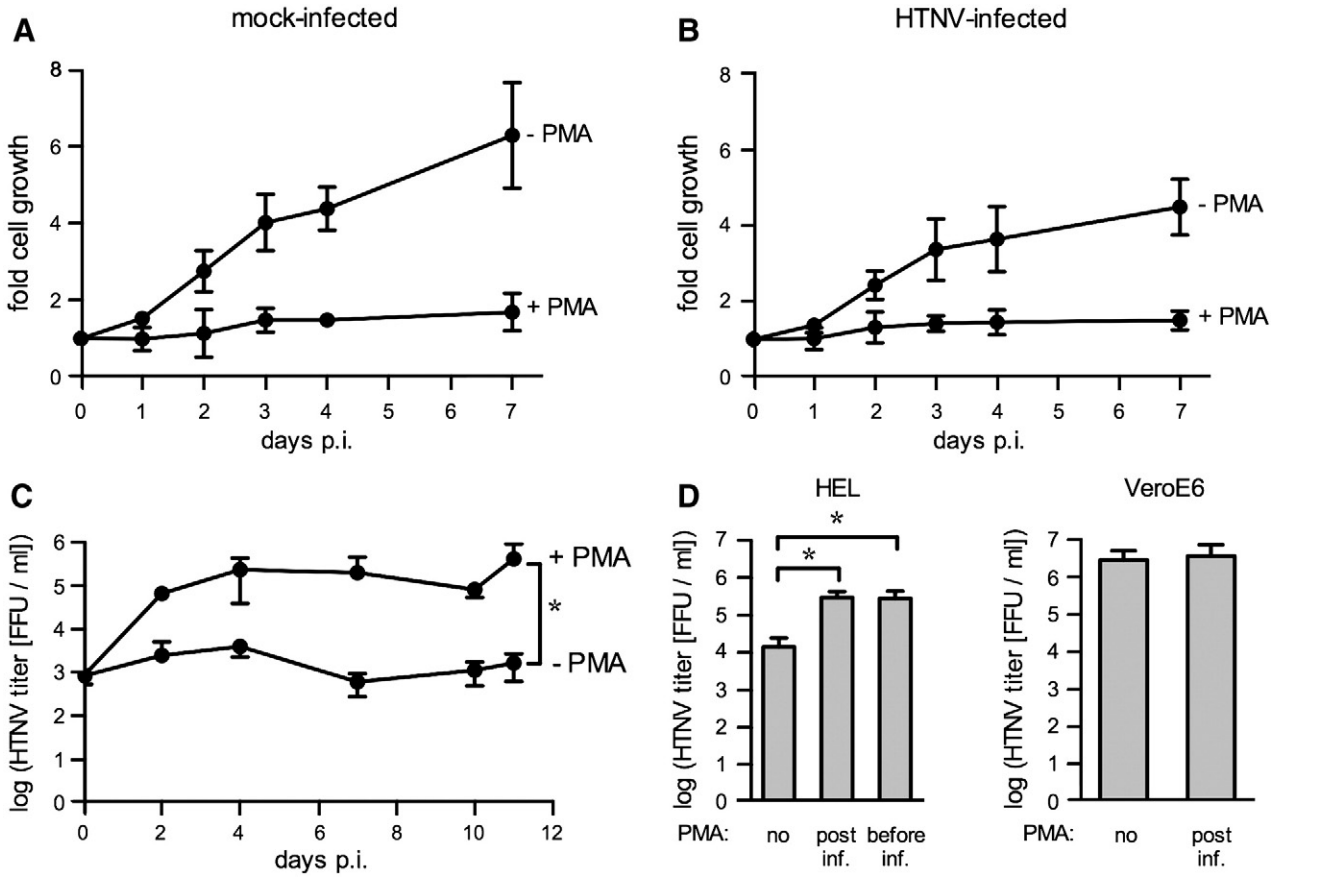

Fig. 3. Cell proliferation arrest and switch to high-level HTNV replication in differentiating megakaryocytic cells. (A) Mock- and (B) HTNV-infected (MOI = 1.5) HEL cells were left unstimulated (−PMA) or stimulated (10 nM PMA at 1 h p.i.). The numbers of live cells were determined by trypan exclusion assay at the time points indicated and is given on the *y*-axis relative to the cell number at time point 0 (fold growth). (C) Virus titers in supernatants from mock-infected and HTNV-infected (MOI = 1.5) HEL cells, either unstimulated (−PMA) or stimulated (10 nM PMA at 1 h p.i.), were analyzed at the time points indicated and are shown as focus-forming units (FFU) per ml on a log scale. (D, left graph) HTNV-infected (MOI = 1.5) HEL cells were left unstimulated or stimulated (10 nM PMA) at either 1 h post or 1 day before infection. At 3 days p.i., virus titers in supernatants were measured. (D, right graph) Virus titers in supernatants from unstimulated or stimulated (10 nM PMA at 1 h p.i.) HTNV-infected Vero E6 cells were determined at 3 days after infection. Results shown are means ± 1 SD derived from 3 independent experiments (*$p<0.05$, Student's *t*-test).

virus titers in the supernatant of HTNV-infected Vero E6 cells (Fig. 3D, right panel).

Collectively, these data show that PMA-induced differentiation of megakaryocytic cells is associated with drastically upregulated release of HTNV virions in the face of arrested cell proliferation.

Unaltered megakaryocyte differentiation despite high-level HTNV replication

Next we analyzed in detail whether the switch to high-level HTNV replication interfered with megakaryocytic differentiation of HEL cells. Fig. 4 shows PMA-induced upregulation of CD41 (integrin IIb) and CD61 (integrin β3) on both mock-infected and HTNV-infected HEL cells. These molecules form αIIbβ3, a heterodimeric receptor that is increasingly expressed on megakaryocytes as they mature (Szalai et al., 2006). In contrast, neither mock-infected nor HTNV-infected HEL cells expressed CD42, a marker of late megakaryopoiesis, after PMA stimulation.

Megakaryocyte differentiation of HEL cell has been shown to result in enhanced adhesion to components of the extracellular matrix including fibrinogen, fibronectin, and vitronectin (Molla et al., 1995; Molla and Block, 2000; Ylanne et al., 1990). Fig. 5A demonstrates that both mock- and HTNV-infected HEL cells adhered more strongly to surfaces coated with fibronectin, vitronectin, or fibrinogen after PMA treatment as compared to unstimulated HEL cells. PMA-treated megakaryocytic cells such as HEL cells do not proliferate but further increase their polyploidy by endoreplication (Long et al., 1990), the continued synthesis of DNA in the absence of mitosis and cytokinesis. We observed that the DNA content of mock-infected and HTNV-infected HEL cells was similar (Fig. 5B and Table 1). Thus, after PMA-induced differentiation polyploidization occurred in HEL cells whether mock-infected or HTNV-infected.

Collectively, these data indicate that PMA-induced differentiation of megakaryocytic cells is not impaired by high-level HTNV replication.

Evasion of type I interferon (IFN)-associated innate responses by HTNV in differentiating megakaryocytic cells

We now investigated innate responses in PMA-treated megakaryocytic cells. For this purpose, quantitative RT-PCR was used to determine the number of transcripts encoding retinoic acid-inducible gene (RIG)-I-like receptors (Fig. 6). They represent IFN-stimulated genes (ISGs) that are upregulated by type I IFN through a positive feedback loop (Yoneyama et al., 2004). After mock-infection untreated as well as PMA-treated HEL cells expressed only very low numbers of transcripts encoding RIG-I or melanoma differentiation-associated gene 5 (MDA5). However, untreated HEL cells upregulated the number of RIG-I and MDA5 transcripts 8 h after infection with Vesicular stomatitis virus (VSV), a strong trigger of innate responses. Intriguingly, this VSV-induced upregulation was drastically enhanced in PMA-treated HEL cells. Moreover, in response to type I IFN PMA-treated HEL cells produced more transcripts encoding RIG-I-like receptors as compared to untreated HEL cells. In contrast, poly I:C had no

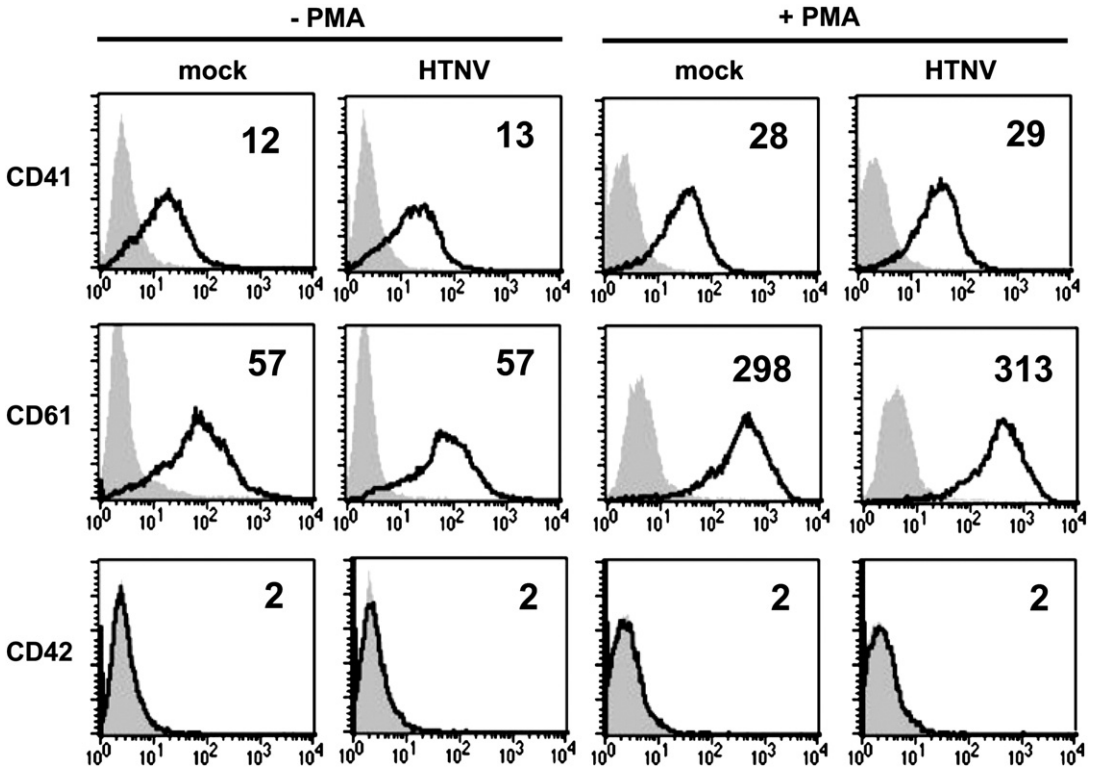

Fig. 4. Expression of differentiation markers on HTNV-infected megakaryocytic cells. Mock- and HTNV-infected (MOI = 1.5) HEL cells were left unstimulated (−PMA) or stimulated (10 nM PMA at 1 h p.i.). At 3 days p.i., cells were stained for CD41, CD61, or CD42. As secondary antibody PE-conjugated anti-mouse IgG was used. Grey filled histograms represent isotype controls, and black histograms show specific staining as indicated (MFI is given in the upper right corner). On the *x*-axis, the fluorescence intensity (log scale, 4 decades) is given, whereas the *y*-axis cell depicts cell counts. One representative experiment out of three is shown.

effect on RIG-I expression. Poly I:C is an agonist of Toll-like receptor 3 (TLR3) that has been shown to detect HTNV (Handke et al., 2009) but was not expressed in HEL cells (data not shown). Most strikingly, HTNV did not induce expression of RIG-I-like receptor transcripts either in untreated or in PMA-treated cells 8 h after infection. Similar results were obtained analyzing other ISGs (interferon regulatory factor 7 and matrix metalloproteinase 9; data not shown).

Next the effect of PMA on RIG-I expression in HEL cells was analyzed on the protein level in the course of four days after HTNV infection (Fig. 7). RIG-I protein was neither upregulated in unstimulated nor in PMA-stimulated megakaryocytic cells. Surprisingly, PMA reduced the amount of RIG-I protein in mock-infected as well as in HTNV-infected HEL cells. Thus, a PMA-associated mechanism interferes with RIG-I expression on the protein level. Such a mechanism could explain at least in part increased HTNV replication in PMA-treated HEL cells as RIG-I serves as a sensor of HTNV replication (Lee et al., submitted).

Collectively, these data demonstrate that HTNV efficiently evades induction of innate responses in untreated as well as in PMA-treated HEL cells despite switch to high-level replication in the latter.

Enhanced expression of HLA class I molecules on differentiating megakaryocytic cells after HTNV infection

Many viruses block expression of HLA class I molecules to escape the attack by cytotoxic T lymphocytes (CTLs) (Hansen and Bouvier, 2009). In contrast, HTNV has been demonstrated to induce HLA class I expression on myeloid dendritic cells (Raftery et al., 2002) and endothelial cells (Geimonen et al., 2002; Kraus et al., 2004). Therefore, we tested whether HTNV influenced the expression of these important antigen presenting molecules on differentiating megakaryocytic cells. For this purpose, PMA-stimulated HEL cells were mock infected, HTNV infected or treated with type I IFN. Subsequently, the surface density of HLA class I molecules was measured by flow cytometry. HTNV upregulated HLA class I molecules on unstimulated HEL cells at 3 days p.i. (see Fig. 8A, left graphs). Intriguingly, the increase of HLA class I molecules on PMA-treated HEL cells after HTNV infection (see Fig. 8A, right graphs, and Fig. 8B) was much stronger and started already at 1 day p.i.

These findings demonstrate that high-level HTNV replication in differentiating megakaryocytic cells strongly upregulates HLA class I molecules on the cell surface.

Discussion

In this study, we demonstrate for the first time that HTNV targets megakaryocytic cells. In striking contrast, TULV and PHV, both rather non-pathogenic hantaviruses, did not multiply in this cell type. After induction of differentiation, HTNV-infected megakaryocytic cells switched to high-level virion production and strongly increased surface expression of HLA class I molecules.

High densities of integrin β1 as well as integrin β3, and CD55/DAF, which facilitate HTNV entry (Gavrilovskaya et al., 1998, 1999; Krautkramer and Zeier, 2008), were found on HEL cells and human primary megakaryocytes. This observation is in line with previous studies demonstrating that HEL cells express several integrin heterodimers including α5β1 (fibronectin receptor), αIIbβ3 (fibrinogen receptor), and αvβ3 (vitronectin receptor) (Ylanne et al., 1990). The integrin heterodimer αIIbβ3 did not bind fluorescence-labeled fibrinogen indicating that it was in an inactive conformation (data not shown). This allows HTNV to bind to plexin–semaphorin–integrin domains which are exposed only on the inactive, bent β3 molecule (Raymond et al., 2005). In contrast, gC1qR which has been reported to enhance entry of HTNV infection into human lung epithelial A549 cells (Choi et al., 2008) was not detected on HEL cells and only weakly expressed by human primary megakaryocytes, suggesting that this receptor is not required for virus entry into megakaryocytic cells.

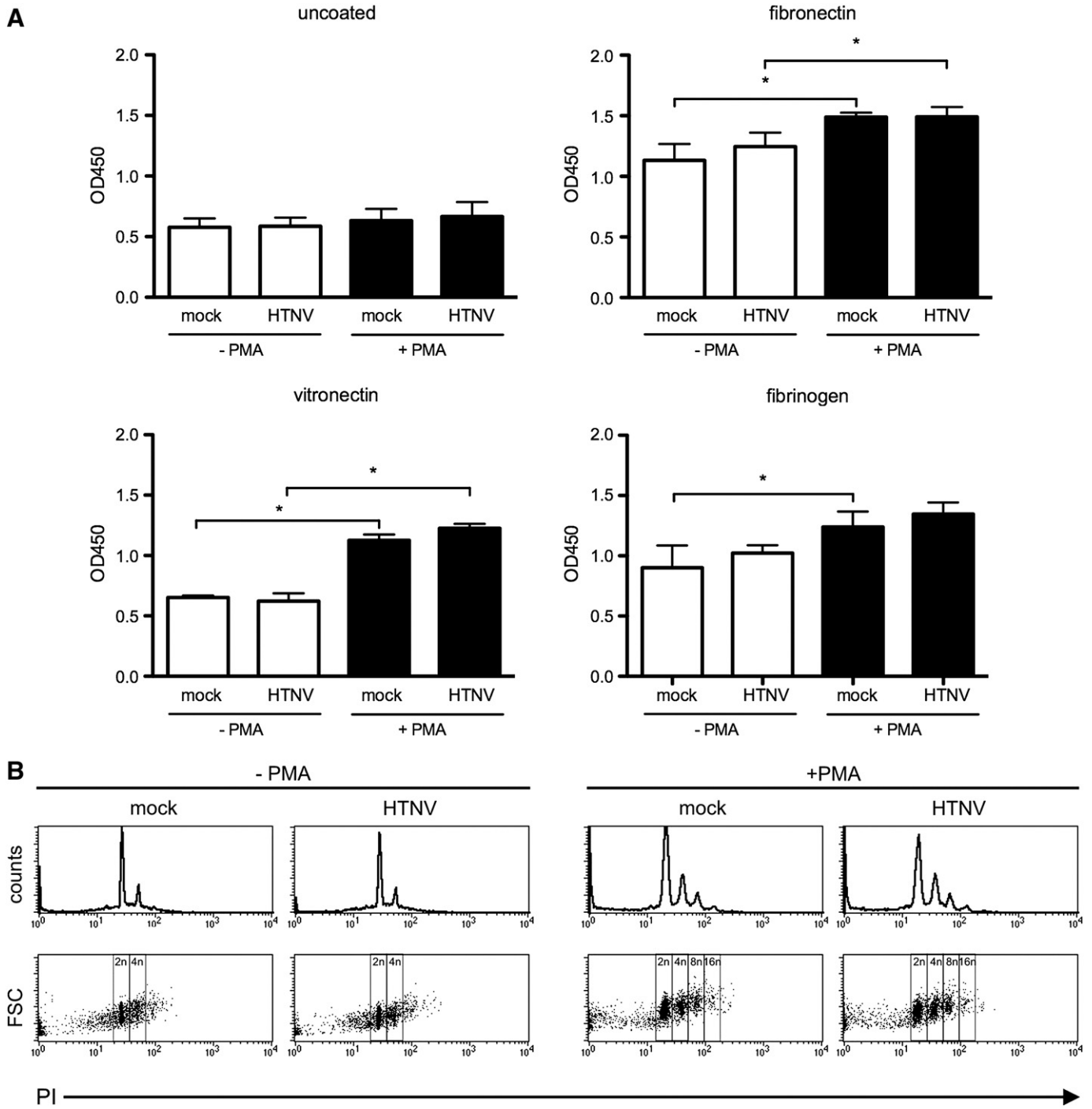

Fig. 5. Adhesion and endoreplication of HTNV-infected differentiating megakaryocytic cells. Mock- and HTNV-infected (MOI = 1.5) HEL cells were left unstimulated (−PMA) or stimulated (10 nM PMA at 1 h p.i.). (A) At 3 days p.i., cells were allowed to adhere to wells that were uncoated or coated with extracellular matrix (ECM) ligands (fibrogen, fibronectin, or vitronectin). After extensive washing, the abundance of cells adhering to ECM ligands was quantified by MTT assay. Results shown are means ± 1 SD of triplicate runs and are derived from three independent experiments (*$p<0.05$, one-way analysis of variance). (B) At 7 days p.i., endoreplication of cells was visualized by cytofluorimetric analysis of propidium iodide staining. Upper row: histogram blots of DNA content in HEL cells; the *x*-axis indicates fluorescence intensity (log scale, 4 decades), whereas the *y*-axis shows cell counts. Lower row: dot blot analyses of DNA content in HEL cells; the *x*-axis indicates fluorescence intensity (log scale, 4 decades), whereas the *y*-axis shows cell size (forward scatter, FSC). Gates mark different stages of DNA ploidy (2n: DNA content of HEL cells in the G_o/G_1 phase; 4n: diploid cells in G_2 phase or early polyploid cells; 8n: a fourfold increase in DNA content; 16n: an eightfold increase in DNA content). One representative experiment out of four independent experiments is shown.

Non-pathogenic TULV and PUUV could not infect HEL cells despite strong surface expression of integrin β1, a receptor for non-pathogenic hantaviruses (Gavrilovskaya et al., 1998, 1999). Previous reports have demonstrated that adhesion of HEL cells to extracellular matrix components is mainly mediated by integrin β1 (Garcia et al., 1998; Molla et al., 1995). This suggests that integrin β1 on HEL cells is in the active conformation and thus cannot mediate entry of TULV and PHV. Alternatively, a hitherto unknown coreceptor required for infection with non-pathogenic hantaviruses is missing on HEL cells. It is also possible that non-pathogenic hantaviruses enter HEL cells but fail to establish a productive infection. Collectively, the selective susceptibility of HEL cells to a pathogenic hantavirus points towards an important role of this cell type in virus-induced pathogenesis.

Table 1
Ploidy analysis of megakaryocytic cells in uninfected or HTNV-infected cell cultures.[a]

Ploidy[b]	No PMA		PMA	
	Uninfected	HTNV infected	Uninfected	HTNV infected
2n	45.5%	43.5%	30.5%	29.8%
4n	19%	18%	16%	17%
8n	—	—	6%	5.8%
16n	—	—	1.5%	1.8%

[a] Ploidy was measured as shown in Fig. 5B. Data are means derived from four independent experiments.
[b] 2n: DNA content of HEL cells in the G_o/G_1 phase; 4n: diploid cells in G_2 phase or early polyploid cells; 8n: a fourfold increase in DNA content; 16n: an eightfold increase in DNA content.

PMA had no effect on virus growth in Vero E6 cells. In striking contrast, in cultures of PMA-treated HEL cells, virus titers increased more than 100-fold compared to untreated HEL cells. On a per cell basis, upregulation of HTNV replication was even more pronounced as HEL cells stopped proliferating after PMA-induced differentiation. In addition, human primary megakaryocytes treated with PMA were efficiently infected with HTNV as demonstrated by strong staining of viral N protein in immunofluorescence microscopy analysis. Similar to HTNV-infected dendritic cells (DCs) (Raftery et al., 2002), endothelial cells (Pensiero et al., 1992; Temonen et al., 1993), Vero E6 cells (Hardestam et al., 2005), and A549 cells (Hardestam et al., 2005) no signs of apoptosis were observed in HTNV-infected HEL cells (data not shown). Overall, these findings suggest that differentiating megakaryocytic cells provide a special environment in which pathogenic hantaviruses can multiply with high efficiency.

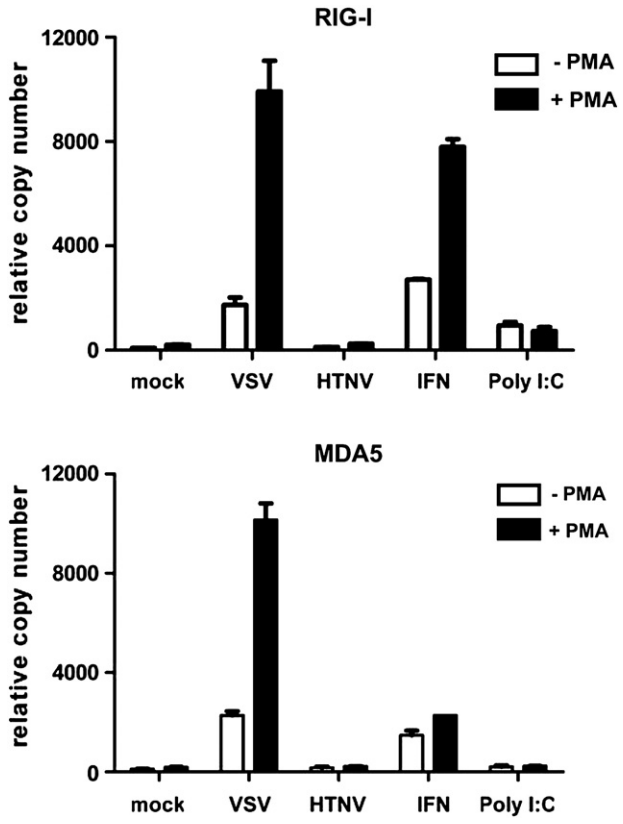

Fig. 6. Expression of RIG-I-like receptors in HTNV-infected HEL cells. HEL cells were left unstimulated (−PMA) or stimulated with 10 nM PMA for 24 h. Thereafter, cells were treated with type I IFN (5000 U/ml), poly I:C (2.5 μg/ml), mock-infected, or infected with either VSV (MOI = 1.5) or HTNV (MOI = 1.5). After 8 h, the relative abundance of transcripts encoding RIG-I (upper graph) or MDA5 (lower graph) was determined by quantitative RT-PCR.

Key marker molecules of megakaryocyte differentiation (Schulze and Shivdasani, 2005) including CD61 (integrin β3), which also serves as a receptor for pathogenic hantaviruses, and CD41 (integrin IIb) were upregulated on both mock- and HTNV-infected HEL cells after PMA stimulation. However, the increase in density of CD61 did not further enhance HNTV entry into HEL cells. Virus titers in the supernatant of HEL cells stimulated with PMA 1 day before infection were as high as those produced by cells treated with PMA 1 h after infection. Adhesion of PMA-treated HEL cells through surface integrins to components of the extracellular matrix, an important step in megakaryocyte differentiation, was not blocked by HTNV. Moreover, high-level HTNV replication did not affect PMA-induced polyploidization in HEL cells. The latter is a characteristic feature of differentiating megakaryocytes and caused by repeated rounds of DNA replication without concomitant cell division (Ravid et al., 2002). In conclusion, megakaryocyte differentiation appeared to proceed normally in HTNV-infected HEL cells.

We found that VSV induced expression of transcripts encoding RIG-I-like receptors in untreated HEL cells at 8 h post-infection. This VSV-induced upregulation was drastically increased in PMA-treated HEL cells. Furthermore, PMA sensitized HEL cells to type I IFN, leading to increased number of transcripts derived from RIG-I-like receptor genes and other ISGs (interferon regulatory factor 7 and matrix metalloproteinase 9; data not shown). Supporting our finding, PMA has been reported to upregulate type I IFN receptor density on the cell surface of human megakaryocytic cells by a post-transcriptional mechanism (Martyre and Wietzerbin, 1994). Moreover, PMA activates the vav proto-oncogene (Gulbins et al., 1994), which is predominantly expressed in cells of the hematopoietic system (Katzav, 1995), and participates in signaling through the type I IFN receptor (Micouin et al., 2000). Cell type specificity of this sensitizing effect is documented by the fact that PMA inhibits type I IFN signaling in human peripheral blood monocytes and fibroblasts (Petricoin et al., 1992, 1996).

In sharp contrast to VSV, HTNV failed to induce ISG transcripts at early time points in untreated and PMA-treated human megakaryocytic cells despite PMA-induced sensitization to type I IFN signaling and high-level virus replication. Previous reports have described evasion of innate responses by pathogenic hantaviruses. HTNV and New York virus (NYV), a pathogenic New World hantavirus, delay type I IFN responses in endothelial cells (Geimonen et al., 2002; Kraus et al., 2004). Subsequently, it has been demonstrated that the G1 cytoplasmic tail of NYV inhibits RIG-I-mediated induction of type I IFN (Alff et al., 2006; Alff et al., 2008). In addition, Andes virus (ANDV), another pathogenic New World hantavirus, interferes with both IFN regulatory factor 3 activation and IFN signaling in endothelial cells (Spiropoulou et al., 2007). Our results extend these findings and show that HTNV efficiently evades induction of ISG transcripts in differentiating megakaryocytic cells.

We observed a slight downregulation of RIG-I on the protein level in PMA-treated HEL cells after mock as well as after HTNV infection. Diminished abundance of RIG-I protein could contribute to enhanced HTNV replication in differentiating megakaryocytic cells because this molecule acts as a cytoplasmic sensor of HTNV replication (Lee et al., submitted). However, the molecular mechanisms underlying the switch to high-level HTNV replication in differentiating megakaryocytic cells remain to be defined.

Most viruses have also evolved sophisticated mechanisms to escape from antiviral T cells by interfering with antigen presentation through the HLA class I pathway (Hansen and Bouvier, 2009). In striking contrast, HTNV has been demonstrated to increase surface expression of HLA class I molecules on dendritic cells (Raftery et al., 2002) and endothelial cells (Geimonen et al., 2002; Kraus et al., 2004). In this study, HTNV infection increased the density of HLA class I proteins on the surface of differentiating megakaryocytic cells. Upregulation of HLA class I molecules was detected on untreated HEL cells at day 3 after HTNV infection. This effect was much stronger and started earlier on PMA-treated HEL cells in parallel with the PMA-induced switch to high-level virus replication. It is unlikely that type I IFN plays a role in HTNV-induced upregulation of HLA

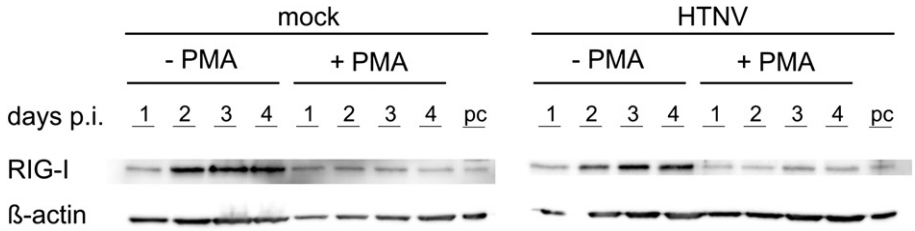

Fig. 7. Western blot analysis of RIG-I expression in mock- and HTNV-infected megakaryocytic cells. HEL cells were left untreated (−PMA) or stimulated with 10 nM PMA (+PMA) at 1 h post-HTNV infection (MOI = 1.5) and mock infection, respectively. Infected cells were harvested at the time points indicated and analyzed by Western blot for RIG-I expression. Huh7 cells stimulated with IFN-α (2000 U/ml) were used as a positive control (pc). As a loading control expression of β-actin was determined. Results shown are representative of three independent experiments.

class I molecules on HEL cells as the virus did not induce ISGs. Possibly, HTNV activates the transcription factor NF-κB which increases transcription of HLA class I molecules as described for West Nile virus infection (Kesson and King, 2001). On the other hand, it has been demonstrated that HTNV N protein sequesters NF-κB in the cytoplasm thereby interfering with NF-κB activity (Taylor et al., 2009). Alternatively, HTNV could modulate HLA class I expression by increasing import of peptides into the ER and assembly of HLA class I proteins similar to West Nile virus (Momburg et al., 2001). The precise mechanisms of HTNV-induced upregulation of HLA class I molecules remain to be defined in future studies.

Initially, HLA class I upregulation could help HTNV to evade the innate response and spread because inhibitory receptors on NK cells are stimulated by HLA class I molecules (Lanier, 2008). Later, virus-induced HLA class I expression could contribute to the elimination of HTNV-infected megakaryocytes during the adaptive phase of the antiviral immune response. Supporting this notion, the efficiency of lysis by CTLs correlates with the strength of HLA class I expression (King et al., 1986; Shimonkevitz et al., 1985).

In conclusion, our results suggest that differentiating megakaryocytic cells represent an important target for pathogenic hantaviruses in humans. Megakaryocyte differentiation remained unaltered despite high-level HTNV replication. Therefore, a direct viral effect on megakaryopoiesis seems unlikely. Intriguingly, HTNV infection of differentiating megakaryocytic cells resulted in strongly enhanced surface expression of HLA class I molecules. This suggests that *in vivo* HTNV-infected megakaryocytes could be efficiently eliminated by antiviral CTLs during differentiation resulting in acute thrombocytopenia. In line with this view, the frequency of virus-specific CTLs has been shown to correlate with the severity of disease in HCPS patients (Kilpatrick et al., 2004). Moreover, immunosuppressive corticosteroid therapy, which suppresses CTL responses, increases platelet counts in NE patients (Dunst et al., 1998; Seitsonen et al., 2006). Finally, a high frequency of virus-specific T cells producing IFN-γ, which controls viral spread through non-cytolytic virus clearance (Guidotti and Chisari, 2001), correlates with less severe HFRS (Wang et al., 2009). Preventing elimination of HTNV-infected megakaryocytes by CTLs might represent an important strategy for treatment of severe hantavirus-induced hemorrhage. The possibility that pathogenic hantaviruses interfere with megakaryopoiesis through immune mechanisms needs to be explored in future animal models of hantavirus-induced human disease.

Materials and methods

Cells and viruses

The megakaryocytic and myeloid cell lines used in this study (HEL, K562, and Meg-01) were maintained in RPMI 1640 supplemented with 10% heat-inactivated fetal calf serum (FCS), 2 mM L-glutamine, penicillin, and streptomycin (PAA, Pasching, Austria). Vero E6 cells were grown in MEM (PAA) supplemented with the same additives. TF-1 cell were maintained in RPMI medium, supplemented with 2 mM L-glutamine, 10% heat-inactivated FCS, and 5 ng/ml recombinant human granulocyte-macrophage colony-stimulating factor (GM-CSF) from Immunotools (Friesoythe, Germany). For infection, HEL cells were incubated with HTNV, which was allowed to adsorb for 60 min at 37 °C. After washing three times with medium, HEL cells were stimulated with 10 nM PMA (Sigma Aldrich, Deisendorf, Germany), 1 h after or 1 day before infection.

HTNV (strain 76-118), TULV (strain Moravia), and PHV (type-3571) were propagated in Vero E6 cells in a biosafety level 3 facility as previously described (Kraus et al., 2004). Briefly, supernatant was collected from cell cultures at 7–10 days p.i., cleared of cell debris by centrifugation at 2000×*g*, aliquoted, and frozen at − 80 °C. Virus stocks were free of mycoplasma as tested by PCR-based VenorGeM mycoplasma detection kit (Minerva Biolabs, Berlin, Germany).

For generation of primary megakaryocytes, 5×10^5 CD34+ cells (purity >90%) were incubated in a 6-well plate in the presence of recombinant human thrombopoietin (10 ng/ml) and IL-1β (10 ng/ml) (both from R&D systems, Wiesbaden, Germany) using STEM span medium (Stemcell technologies, Köln, Germany) supplemented with 1 mM sodium pyruvate and 1× non-essential amino acids for 7–12 days at 37 °C in a humidified incubator with 5% CO_2. On day 5, large cells were readily present in the culture and recognized as megakaryocytes.

Virus titration

Hantavirus titers were determined as described recently (Heider et al., 2001). Briefly, Vero E6 cells were infected by serial dilutions of supernatants for 1 h to allow absorbance of virus particles. Thereafter, cells were overlaid with medium containing 0.5% agarose. After 7 days of incubation at 37 °C, the overlay was removed and cells were washed with PBS and fixed with methanol for 10 min. After incubation with a hantavirus N protein-specific polyclonal rabbit serum the SuperSignal West Dura Extended Duration Substrate kit (Pierce/Perbio, Bonn, Germany) was used according to the manufacturer's instructions to visualize antigen-positive foci. Finally, the antigen-positive foci were counted to calculate virus titers, which are expressed as focus-forming units per ml.

Western blot

HEL cells were lysed in lysis buffer containing 250 mM Tris, 2% SDS, 10% glycerol, 5% mercaptoethanol, and 0.01% bromophenol blue followed by heat-denaturation of the sample for 5 min at 95 °C. Proteins were separated by 10% sodium dodecyl sulfate (SDS)–polyacrylamide gel electrophoresis and transferred onto a PVDF membrane (Millipore, Schwalbach, Germany) followed by blocking with 5% milk powder for 1 h. The membrane was incubated with primary antibody at 4 °C overnight. RIG-I and β-actin-specific antibodies were purchased from Alexis Biochemicals (Grünberg, Germany). For detection of primary antibodies, an anti-rabbit or anti-mouse peroxidase-conjugated antibody (Amersham, Freiburg,

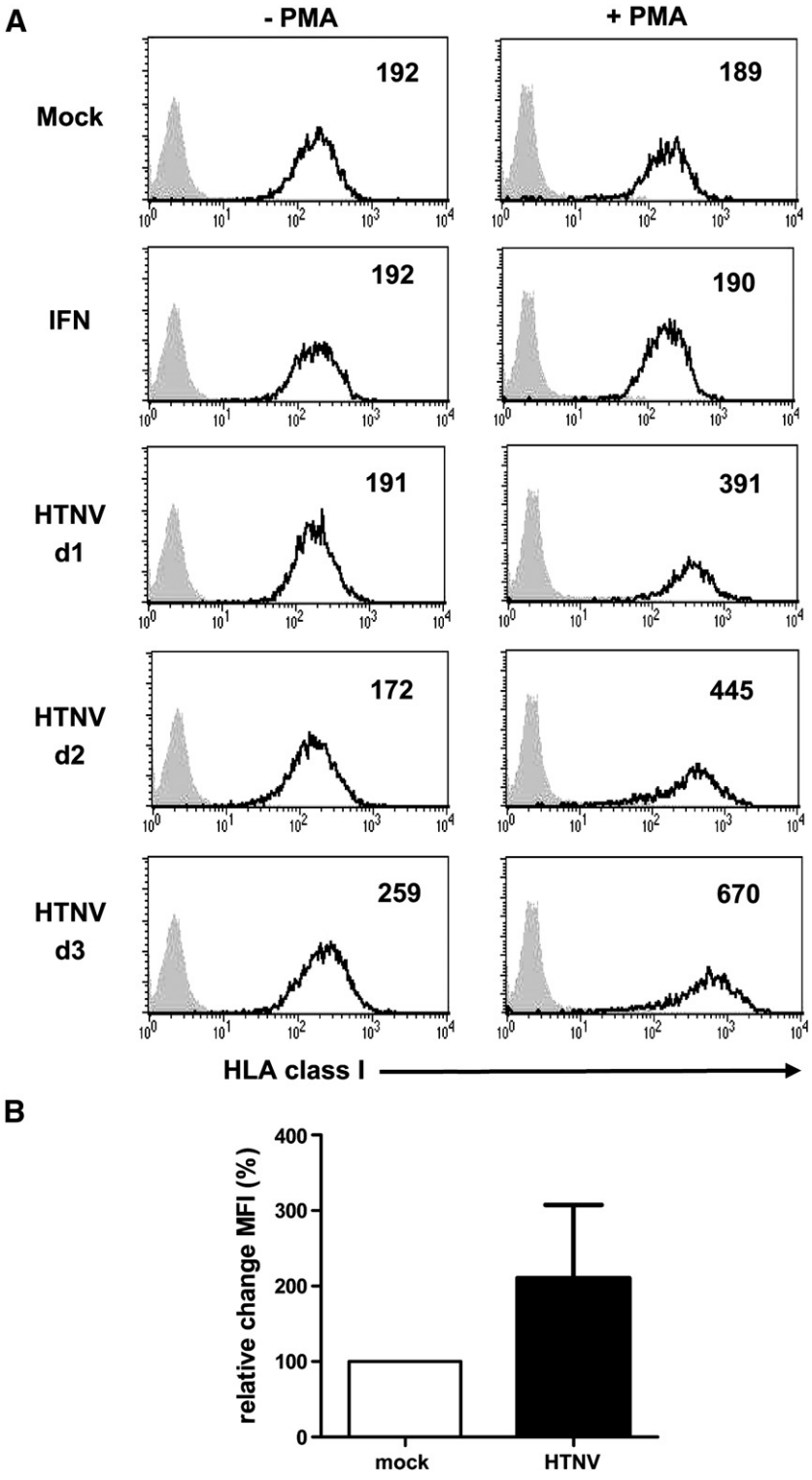

Fig. 8. HTNV-induced upregulation of HLA class I molecules. HEL cells were either left unstimulated (−PMA) or stimulated (10 nM PMA at 1 h p.i.) after mock infection, treatment with IFN-α (5000 U/ml for 24 h), or HTNV infection (MOI = 1.5). (A) Time course of HTNV-induced HLA class I upregulation. Grey filled histograms represent isotype controls, and black curves show specific staining for HLA class I proteins. The mean fluorescence intensity (MFI) is given in the upper right corner. On the *x*-axis, the fluorescence intensity (log scale, 4 decades) is given, whereas the *y*-axis cell depicts cell counts. One representative experiment out of two is shown. (B) Relative change in MFI of HLA class I expression after HTNV infection. HEL cells stimulated with PMA (10 nM PMA at 1 h p.i.) were either mock-infected or infected with HTNV for 3 days before FACS analysis (MFI of mock-infected cells was set 100%; $n = 4$).

Germany) was used. Western blots were developed by using SuperSignal West Dura Extended Duration Substrate kit from Pierce/Perbio (Bonn, Germany) according to the manufacturer's protocol.

Immunofluorescence

Cover slides were washed twice with water and rinsed with 70% ethanol. After drying, cover slides were coated with poly-L-lysine

(Biochrom, Berlin, Germany), incubated at 37 °C for 30 min and subsequently washed twice with water. Cells were harvested and washed three times, resuspended in medium and allowed to adhere to poly-L-lysine-coated cover slides for 15 min at 37 °C. Cells were either fixed with acetone/methanol for 10 min or with 4% formaldehyde for 60 min. Formaldehyde-fixed cells were permeabilized with 0.1% Triton for 5 min and washed in PBS three times. Before staining cells were incubated in blocking solution (PBS with 1% FCS) for 30 min at 4 °C followed by three washing steps in PBS. Thereafter, cover slides were incubated in a dark moist chamber for 1 h at 37 °C with primary antibodies that had been diluted in PBS containing 10% heat-inactivated FCS. After washing, bound primary antibodies were visualized by fluorescein isothiocyanate (FITC)-conjugated or Texas Red-conjugated secondary antibodies (1:400).

LightCycler quantitative RT-PCR

Cells were lysed with MagNA Pure lysis buffer (Roche, Mannheim, Germany) and mRNA was isolated with a MagNA Pure-LC device using standard protocols. RNA was reverse-transcribed with AMV-RT and oligo (dT) primer using the First Strand cDNA Synthesis Kit from Roche (Mannheim, Germany). For amplification of target sequences, LightCycler Primer Sets (Search-LC, Heidelberg, Germany) were used with LightCycler FastStart DNA Sybr Green I Kit (Roche, Mannheim, Germany). RNA input was normalized by the average expression of the housekeeping genes encoding β-actin and cyclophilin B. By plotting a known input concentration of a plasmid to the PCR cycle number at which the detected fluorescence intensity reached a fixed value, a virtual standard curve was generated. This standard curve was used to calculate transcript copy numbers. The presented relative copy numbers are mean averages of data of two independent analyses for each sample and parameter.

Flow cytometry

For surface staining, cells were harvested and washed twice in ice-cold FACS washing solution (PBS with 1% heat-inactivated FCS and 0.02% sodium azide). Thereafter, cells were resuspended in 50 µl FACS blocking solution (PBS with 10% heat-inactivated FCS and 0.2% sodium azide) containing primary antibody and incubated for 1 h. The following primary antibodies were used: anti-β1 (clone MEM-101A from Immunotools, Friesoythe, Germany), anti-β3 (clone C17 from Immunotools), anti-CD55/DAF (clone 143-30 from Southern Biotechnology associates, Birmingham, USA), anti-CD41 (clone MEM-06 from Immunotools), and anti-CD42 (clone HIP1 from Immunotools). After incubation, cells were again washed with FACS wash solution and for visualization PE- or FITC-coupled goat anti-mouse antibodies (Dianova, Hamburg, Germany) diluted in FACS block solution were added. After 45 min, the cells were washed with FACS wash solution and resuspended in FACS fixation solution (0.5 ml PBS with 0.37% formaldehyde). For quantifying fluorescence of labeled cells, a FACsCalibur (Becton Dickinson, Heidelberg, Germany) was used. Results were evaluated with the flow cytometry analysis software program CellQuest Pro (BD Bioscience, Heidelberg, Germany).

Adhesion assay

For testing adhesion of HEL cells, uncoated 96-well plates (Sarstedt, Nürnberg, Germany) were coated with 10 µg/ml fibrinogen (Invitrogen, Karlsruhe, Germany), 10 µg/ml fibronectin (Invitrogen), or 0.5 µg/ml vitronectin (Sigma Aldrich, Deisendorf, Germany) at 4 °C overnight. After washing off ligands three times with PBS, wells were coated with coating buffer (PBS with 0.05% BSA) for 60 min at 37 °C. HEL cells that had been infected with HTNV and harvested 3 days p.i. were adjusted to 5×10^4 cells/well and allowed to adhere to ligands for 90 min. Non-adherent cells were washed off three times with PBS. For quantifying the number of adherent cells, the EZ4U Cell Proliferation Assay from Biomedica (Vienna, Austria) was used. This assay is based on the fact that living cells metabolize tetrazolium salt into its deep red colored formazan derivative. After adherent HEL cells were covered with 200 µl cell culture medium, 20 µl of dye substrate was added and optical density was recorded 3 h later at 450 nm.

Cell proliferation

For differentiating between dead and live cells, a 0.5% trypan blue solution was used. Ten microliters of the cell dilution was filled into a hematocytometer chamber. Dead and live cells in one big square (16 small squares) were counted and cell number was determined according to the following formula: cells × dilution factor × 10^4 = cells/ ml.

Endoreplication

HEL cells were harvested and adjusted to 1×10^6 cells/ml. After fixation in ice-cold 70% ethanol, cells were washed with PBS. RNA was digested with DNase- and protease-free RNase A (Qiagen, Hilden, Germany) for 30 min at 50 µg/ml. Propidium iodide (Roth, Karlsruhe, Germany) was added 20 min prior to FACS analysis at 50 µg/ml to determine the DNA content.

Acknowledgments

We thank T. Kaiser (Deutsches Rheumaforschungszentrum) for assistance in flow cytometry, Å. Lundkvist (Swedish Institute for Infectious Disease Control) for hantaviruses (HTNV, TULV), R. B. Tesh (University of Texas) for PHV, A. Rang (Charité-Universitätsmedizin Berlin) for focus-purified PHV, and C. Priemer (Charité-Universitätsmedizin Berlin) for cultivation of Vero E6 cells. This work was supported by grants from the Deutsche Forschungsgemeinschaft (GraKo 1121 to M.-H. L., N. L., and P. L.).

References

Alff, P.J., Gavrilovskaya, I.N., Gorbunova, E., Endriss, K., Chong, Y., Geimonen, E., Sen, N., Reich, N.C., Mackow, E.R., 2006. The pathogenic NY-1 hantavirus G1 cytoplasmic tail inhibits RIG-I- and TBK-1-directed interferon responses. J. Virol. 80, 9676–9686.

Alff, P.J., Sen, N., Gorbunova, E., Gavrilovskaya, I.N., Mackow, E.R., 2008. The NY-1 hantavirus Gn cytoplasmic tail coprecipitates TRAF3 and inhibits cellular interferon responses by disrupting TBK1–TRAF3 complex formation. J. Virol. 82, 9115–9122.

Berthier, R., Jacquier-Sarlin, M., Schweitzer, A., Block, M.R., Molla, A., 1998. Adhesion of mature polyploid megakaryocytes to fibronectin is mediated by beta 1 integrins and leads to cell damage. Exp. Cell Res. 242, 315–327.

Chang, B., Crowley, M., Campen, M., Koster, F., 2007. Hantavirus cardiopulmonary syndrome. Semin. Respir. Crit. Care Med. 28, 193–200.

Choi, Y., Kwon, Y.C., Kim, S.I., Park, J.M., Lee, K.H., Ahn, B.Y., 2008. A hantavirus causing hemorrhagic fever with renal syndrome requires gC1qR/p32 for efficient cell binding and infection. Virology 381, 178–183.

Cosgriff, T.M., 1991. Mechanisms of disease in Hantavirus infection: pathophysiology of hemorrhagic fever with renal syndrome. Rev. Infect. Dis. 13, 97–107.

Cosgriff, T.M., Lee, H.W., See, A.F., Parrish, D.B., Moon, J.S., Kim, D.J., Lewis, R.M., 1991. Platelet dysfunction contributes to the haemostatic defect in haemorrhagic fever with renal syndrome. Trans. R. Soc. Trop. Med. Hyg. 85, 660–663.

Dunst, R., Mettang, T., Kuhlmann, U., 1998. Severe thrombocytopenia and response to corticosteroids in a case of nephropathia epidemica. Am. J. Kidney Dis. 31, 116–120.

Edgar, B.A., Orr-Weaver, T.L., 2001. Endoreplication cell cycles: more for less. Cell 105, 297–306.

Garcia, A.J., Takagi, J., Boettiger, D., 1998. Two-stage activation for alpha5beta1 integrin binding to surface-adsorbed fibronectin. J. Biol. Chem. 273, 34710–34715.

Gavrilovskaya, I.N., Shepley, M., Shaw, R., Ginsberg, M.H., Mackow, E.R., 1998. beta3 Integrins mediate the cellular entry of hantaviruses that cause respiratory failure. Proc. Natl Acad. Sci. USA 95, 7074–7079.

Gavrilovskaya, I.N., Brown, E.J., Ginsberg, M.H., Mackow, E.R., 1999. Cellular entry of hantaviruses which cause hemorrhagic fever with renal syndrome is mediated by beta3 integrins. J. Virol. 73, 3951–3959.

Gavrilovskaya, I.N., Gorbunova, E.E., Mackow, N.A., Mackow, E.R., 2008. Hantaviruses direct endothelial cell permeability by sensitizing cells to the vascular permeability factor, VEGF, while angiopoietin-1 and sphingosine 1-phosphate inhibit hantavirus-directed permeability. J. Virol. 82, 5797–5806.

Geimonen, E., Neff, S., Raymond, T., Kocer, S.S., Gavrilovskaya, I.N., Mackow, E.R., 2002. Pathogenic and nonpathogenic hantaviruses differentially regulate endothelial cell responses. Proc. Natl Acad. Sci. USA 99, 13837–13842.

Guidotti, L.G., Chisari, F.V., 2001. Noncytolytic control of viral infections by the innate and adaptive immune response. Annu. Rev. Immunol. 19, 65–91.

Gulbins, E., Coggeshall, K.M., Baier, G., Telford, D., Langlet, C., Baier-Bitterlich, G., Bonnefoy-Berard, N., Burn, P., Wittinghofer, A., Altman, A., 1994. Direct stimulation of Vav guanine nucleotide exchange activity for Ras by phorbol esters and diglycerides. Mol. Cell. Biol. 14, 4749–4758.
Handke, W., Oelschlegel, R., Frank, R., Krüger, D.H., Rang, A., 2009. Hantaan virus triggers TLR-dependent innate immune responses. J. Immunol. 182, 2849–2858.
Hansen, T.H., Bouvier, M., 2009. MHC class I antigen presentation: learning from viral evasion strategies. Nat. Rev. Immunol. 9, 503–513.
Hardestam, J., Klingstrom, J., Mattsson, K., Lundkvist, A., 2005. HFRS causing hantaviruses do not induce apoptosis in confluent Vero E6 and A-549 cells. J. Med. Virol. 76, 234–240.
Heider, H., Ziaja, B., Priemer, C., Lundkvist, A., Neyts, J., Kruger, D.H., Ulrich, R., 2001. A chemiluminescence detection method of hantaviral antigens in neutralisation assays and inhibitor studies. J. Virol. Meth. 96, 17–23.
Hippenstiel, S., Suttorp, N., 2003. Interaction of pathogens with the endothelium. Thromb. Haemost. 89, 18–24.
Jiang, F., Jia, Y., Cohen, I., 2002. Fibronectin- and protein kinase C-mediated activation of ERK/MAPK are essential for proplateletlike formation. Blood 99, 3579–3584.
Katzav, S., 1995. Vav: Captain Hook for signal transduction? Crit. Rev. Oncog. 6, 87–97.
Kaushansky, K., 2005. The molecular mechanisms that control thrombopoiesis. J. Clin. Invest. 115, 3339–3347.
Kesson, A.M., King, N.J., 2001. Transcriptional regulation of major histocompatibility complex class I by flavivirus West Nile is dependent on NF-kappaB activation. J. Infect. Dis. 184, 947–954.
Khaiboullina, S.F., Netski, D.M., Krumpe, P., St Jeor, S.C., 2000. Effects of tumor necrosis factor alpha on sin nombre virus infection in vitro. J. Virol. 74, 11966–11971.
Kilpatrick, E.D., Terajima, M., Koster, F.T., Catalina, M.D., Cruz, J., Ennis, F.A., 2004. Role of specific CD8+ T cells in the severity of a fulminant zoonotic viral hemorrhagic fever, hantavirus pulmonary syndrome. J. Immunol. 172, 3297–3304.
King, N.J., Mullbacher, A., Blanden, R.V., 1986. Relationship between surface H-2 concentration, size of different target cells, and lysis by cytotoxic T cells. Cell. Immunol. 98, 525–532.
Kraus, A.A., Raftery, M.J., Giese, T., Ulrich, R., Zawatzky, R., Hippenstiel, S., Suttorp, N., Kruger, D.H., Schonrich, G., 2004. Differential antiviral response of endothelial cells after infection with pathogenic and nonpathogenic hantaviruses. J. Virol. 78, 6143–6150.
Krautkramer, E., Zeier, M., 2008. Hantavirus causing hemorrhagic fever with renal syndrome enters from the apical surface and requires decay-accelerating factor (DAF/CD55). J. Virol. 82, 4257–4264.
Kruger, D.H., Ulrich, R., Lundkvist, A.H., 2001. Hantavirus infections and their prevention. Microbes Infect. 3, 1129–1144.
Lanier, L.L., 2008. Evolutionary struggles between NK cells and viruses. Nat. Rev. Immunol. 8, 259–268.
Lee, M., 1987. Coagulopathy in patients with hemorrhagic fever with renal syndrome. J. Korean Med. Sci. 2, 201–211.
Long, M.W., Heffner, C.H., Williams, J.L., Peters, C., Prochownik, E.V., 1990. Regulation of megakaryocyte phenotype in human erythroleukemia cells. J. Clin. Invest. 85, 1072–1084.
Martyre, M.C., Wietzerbin, J., 1994. Characterization of specific functional receptors for HuIFN-alpha on a human megakaryocytic cell line (Dami): expression related to differentiation. Br. J. Haematol. 86, 244–252.
Micouin, A., Wietzerbin, J., Steunou, V., Martyre, M.C., 2000. p95(vav) associates with the type I interferon (IFN) receptor and contributes to the antiproliferative effect of IFN-alpha in megakaryocytic cell lines. Oncogene 19, 387–394.
Molla, A., Block, M.R., 2000. Adherence of human erythroleukemia cells inhibits proliferation without inducing differentiation. Cell Growth Differ. 11, 83–90.
Molla, A., Berthier, R., Chapel, A., Schweitzer, A., Andrieux, A., 1995. Beta 1 integrins mediate adherent phenotype of human erythroblastic cell lines after phorbol 12-myristate 13-acetate induction. Biochem. J. 309 (Pt 2), 491–497.
Momburg, F., Mullbacher, A., Lobigs, M., 2001. Modulation of transporter associated with antigen processing (TAP)-mediated peptide import into the endoplasmic reticulum by flavivirus infection. J. Virol. 75, 5663–5671.
Ogawa, M., 1993. Differentiation and proliferation of hematopoietic stem cells. Blood 81, 2844–2853.
Pensiero, M.N., Sharefkin, J.B., Dieffenbach, C.W., Hay, J., 1992. Hantaan virus infection of human endothelial cells. J. Virol. 66, 5929–5936.
Petricoin III, E.F., Hackett, R.H., Akai, H., Igarashi, K., Finbloom, D.S., Larner, A.C., 1992. Modulation of interferon signaling in human fibroblasts by phorbol esters. Mol. Cell. Biol. 12, 4486–4495.
Petricoin III, E., David, M., Igarashi, K., Benjamin, C., Ling, L., Goelz, S., Finbloom, D.S., Larner, A.C., 1996. Inhibition of alpha interferon but not gamma interferon signal transduction by phorbol esters is mediated by a tyrosine phosphatase. Mol. Cell. Biol. 16, 1419–1424.
Raftery, M.J., Kraus, A.A., Ulrich, R., Kruger, D.H., Schonrich, G., 2002. Hantavirus infection of dendritic cells. J. Virol. 76, 10724–10733.
Ravid, K., Lu, J., Zimmet, J.M., Jones, M.R., 2002. Roads to polyploidy: the megakaryocyte example. J. Cell. Physiol. 190, 7–20.
Raymond, T., Gorbunova, E., Gavrilovskaya, I.N., Mackow, E.R., 2005. Pathogenic hantaviruses bind plexin–semaphorin–integrin domains present at the apex of inactive, bent alphavbeta3 integrin conformers. Proc. Natl Acad. Sci. USA 102, 1163–1168.
Saito, H., 1997. Megakaryocytic cell lines. Bailliere's Clin. Haematol. 10, 47–63.
Schmaljohn, C., Hjelle, B., 1997. Hantaviruses: a global disease problem. Emerg. Infect. Dis. 3, 95–104.
Schmaljohn, C.S., Nichol, S.T., 2007. Bunyaviridae. In: Knipe, D.M., Howley, P.M. (Eds.), Fields Virology. Lippencott Williams & Wilkins, Philadelphia, pp. 1741–1789.
Schonrich, G., Rang, A., Lutteke, N., Raftery, M.J., Charbonnel, N., Ulrich, R.G., 2008. Hantavirus-induced immunity in rodent reservoirs and humans. Immunol. Rev. 225, 163–189.
Schulze, H., Shivdasani, R.A., 2005. Mechanisms of thrombopoiesis. J. Thromb. Haemost. 3, 1717–1724.
Seitsonen, E., Hynninen, M., Kolho, E., Kallio-Kokko, H., Pettila, V., 2006. Corticosteroids combined with continuous veno-venous hemodiafiltration for treatment of hantavirus pulmonary syndrome caused by Puumala virus infection. Eur. J. Clin. Microbiol. Infect. Dis. 25, 261–266.
Shimonkevitz, R., Luescher, B., Cerottini, J.C., MacDonald, H.R., 1985. Clonal analysis of cytolytic T lymphocyte-mediated lysis of target cells with inducible antigen expression: correlation between antigen density and requirement for Lyt-2/3 function. J. Immunol. 135, 892–899.
Spiropoulou, C.F., Albarino, C.G., Ksiazek, T.G., Rollin, P.E., 2007. Andes and Prospect Hill hantaviruses differ in early induction of interferon although both can downregulate interferon signaling. J. Virol. 81, 2769–2776.
Sundstrom, J.B., McMullan, L.K., Spiropoulou, C.F., Hooper, W.C., Ansari, A.A., Peters, C.J., Rollin, P.E., 2001. Hantavirus infection induces the expression of RANTES and IP-10 without causing increased permeability in human lung microvascular endothelial cells. J. Virol. 75, 6070–6085.
Szalai, G., LaRue, A.C., Watson, D.K., 2006. Molecular mechanisms of megakaryopoiesis. Cell. Mol. Life Sci. 63, 2460–2476.
Taylor, S.L., Frias-Staheli, N., Garcia-Sastre, A., Schmaljohn, C.S., 2009. Hantaan virus nucleocapsid protein binds to importin alpha proteins and inhibits tumor necrosis factor alpha-induced activation of nuclear factor kappa B. J. Virol. 83, 1271–1279.
Temonen, M., Vapalahti, O., Holthofer, H., Brummer-Korvenkontio, M., Vaheri, A., Lankinen, H., 1993. Susceptibility of human cells to Puumala virus infection. J. Gen. Virol. 74 (Pt 3), 515–518.
Wang, M., Wang, J., Zhu, Y., Xu, Z., Yang, K., Yang, A., Jin, B., 2009. Cellular immune response to Hantaan virus nucleocapsid protein in the acute phase of hemorrhagic fever with renal syndrome: correlation with disease severity. J. Infect. Dis. 199, 188–195.
Yanagihara, R., Silverman, D.J., 1990. Experimental infection of human vascular endothelial cells by pathogenic and nonpathogenic hantaviruses. Arch. Virol. 111, 281–286.
Ylanne, J., Cheresh, D.A., Virtanen, I., 1990. Localization of beta 1, beta 3, alpha 5, alpha v, and alpha IIb subunits of the integrin family in spreading human erythroleukemia cells. Blood 76, 570–577.
Yoneyama, M., Kikuchi, M., Natsukawa, T., Shinobu, N., Imaizumi, T., Miyagishi, M., Taira, K., Akira, S., Fujita, T., 2004. The RNA helicase RIG-I has an essential function in double-stranded RNA-induced innate antiviral responses. Nat. Immunol. 5, 730–737.
Zaki, S.R., Greer, P.W., Coffield, L.M., Goldsmith, C.S., Nolte, K.B., Foucar, K., Feddersen, R.M., Zumwalt, R.E., Miller, G.L., Khan, A.S., 1995. Hantavirus pulmonary syndrome. Pathogenesis of an emerging infectious disease. Am. J. Pathol. 146, 552–579.